Cell Reports
Article

Npas4 Regulates Mdm2 and thus Dcx in Experience-Dependent Dendritic Spine Development of Newborn Olfactory Bulb Interneurons

Sei-ichi Yoshihara,[1,4] Hiroo Takahashi,[1,4] Nobushiro Nishimura,[1] Masahito Kinoshita,[1] Ryo Asahina,[1] Michiko Kitsuki,[1] Kana Tatsumi,[1] Yoko Furukawa-Hibi,[2] Hirokazu Hirai,[3] Taku Nagai,[2] Kiyofumi Yamada,[2] and Akio Tsuboi[1,*]
[1]Laboratory for Molecular Biology of Neural System, Advanced Medical Research Center, Nara Medical University, 840 Shijo-cho, Kashihara, Nara 634-8521, Japan
[2]Department of Neuropsychopharmacology and Hospital Pharmacy, Nagoya University Graduate School of Medicine, Nagoya 466-8560, Japan
[3]Department of Neurophysiology, Gunma University Graduate School of Medicine, Gunma 371-8511, Japan
[4]Co-first author
*Correspondence: atsuboi@naramed-u.ac.jp
http://dx.doi.org/10.1016/j.celrep.2014.06.056

SUMMARY

Sensory experience regulates the development of various brain structures, including the cortex, hippocampus, and olfactory bulb (OB). Little is known about how sensory experience regulates the dendritic spine development of OB interneurons, such as granule cells (GCs), although it is well studied in mitral/tufted cells. Here, we identify a transcription factor, *Npas4*, which is expressed in OB GCs immediately after sensory input and is required for dendritic spine formation. *Npas4* overexpression in OB GCs increases dendritic spine density, even under sensory deprivation, and rescues reduction of dendrite spine density in the *Npas4* knockout OB. Furthermore, loss of *Npas4* upregulates expression of the E3-ubiquitin ligase *Mdm2*, which ubiquitinates a microtubule-associated protein Dcx. This leads to reduction in the dendritic spine density of OB GCs. Together, these findings suggest that Npas4 regulates *Mdm2* expression to ubiquitinate and degrade Dcx during dendritic spine development in newborn OB GCs after sensory experience.

INTRODUCTION

Olfactory bulb (OB) interneurons are a good model for studying the modification of neural circuits by sensory inputs from the external world during the postnatal stages (Katz and Shatz, 1996; Lepousez et al., 2013; Nithianantharajah and Hannan, 2006; Sanes and Lichtman, 2001). OB interneurons are generated and integrated into preexisting neural circuits throughout life (Adam and Mizrahi, 2010; Kaneko et al., 2010; Lledo et al., 2008; Sakamoto et al., 2011; Whitman and Greer, 2009). Newborn interneurons are generated in the subventricular zone, migrate along the rostral migratory stream (RMS), and differentiate into GABA (γ-aminobutyric acid)-releasing inhibitory interneurons, such as granule cells (GCs) and periglomerular cells (PGCs), in the OB (Adam and Mizrahi, 2010; Kaneko et al., 2010; Lledo et al., 2008; Sakamoto et al., 2011; Whitman and Greer, 2009) (Figure 1A). Importantly, adult-born OB interneurons are required for signal processing in a subset of olfactory discrimination learning tasks (Alonso et al., 2012; Bardy et al., 2010). Odor-evoked activity affects the survival and integration of newborn OB interneurons (Lin et al., 2010; Rochefort et al., 2002; Yamaguchi and Mori, 2005). Moreover, olfactory sensory deprivation, or an odor-rich environment, can promote the suppression or acceleration of dendritic morphogenesis and spine formation in newborn OB interneurons, respectively (Livneh et al., 2009; Saghatelyan et al., 2005). These results suggest that olfactory sensory experience facilitates survival, dendritic morphogenesis, and spine formation in OB interneurons. Recently, we found that the 5T4 glycoprotein regulates the dendritic arborization of OB GCs in a sensory-input-dependent manner (Yoshihara et al., 2012). However, little is known about the other molecular players or the precise mechanisms that integrate odor-induced activity with the developmental processes of OB interneurons.

In this study, a unilateral naris occlusion was used in combination with in situ hybridization (ISH) to search for genes whose expression levels differed between the open and closed sides of the OB and whose expression were detected in the interneurons. These experiments identified the *neuronal Per/Arnt/Sim* (*PAS*) *domain protein 4* (*Npas4*) gene (Figure S1A). Npas4 is a helix-loop-helix transcription factor containing two PAS domains and plays a role in the development of inhibitory synapses by regulating the expression of activity-dependent genes in hippocampal neurons (Lin et al., 2008). In addition, Npas4 promotes the formation of inhibitory synapses in the developing visual system (Lin et al., 2008) and controls the homeostatic inhibitory/excitatory balance that regulates visual cortical plasticity (Maya-Vetencourt et al., 2012). Moreover, Npas4 interacts with several promoters that are regulated by neuronal activity (Kim et al., 2010) and mediates the *brain derived neurotrophic factor*

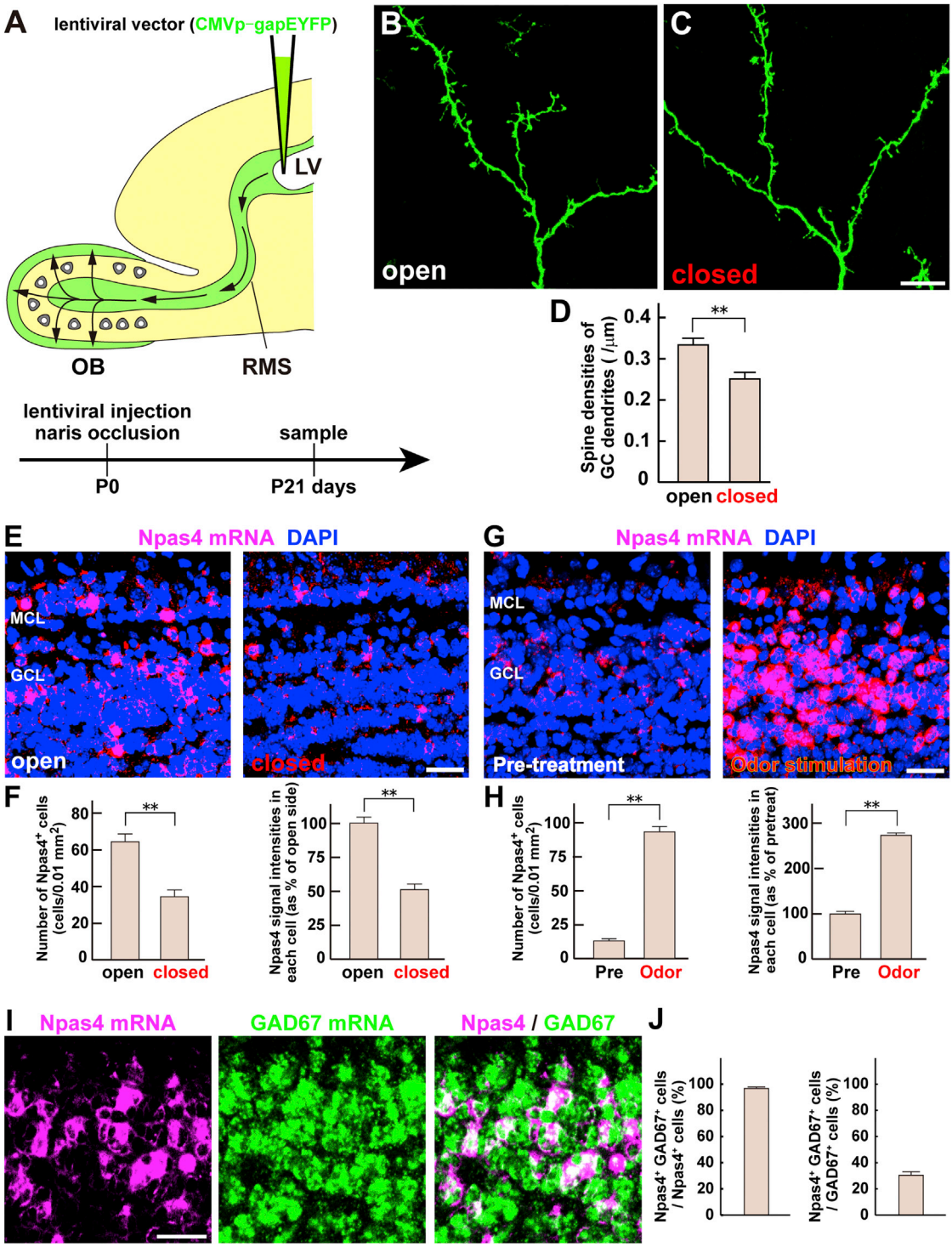

Figure 1. *Npas4* Is Expressed in a Subset of OB GCs in a Sensory-Input-Dependent Manner

(A) Schematic diagram of the experimental protocol. A lentiviral vector carrying the *CMVp—gapEYFP* construct was injected into the LVs of neonatal mice at P0, followed by a unilateral naris occlusion. EYFP$^+$ interneurons in the OB were analyzed 3 weeks (P21) after injection.

(B and C) Newborn GC dendrites in the open (B) and closed (C) sides of the OB of P21 naris-occluded mice. The scale bar represents 10 μm.

(D) Quantification of the spine density (B and C) of GC dendrites. Bars and error bars represent mean ± SEM (open = 0.33 ± 0.02/μm, closed = 0.25 ± 0.02/μm; **$p < 0.01$ compared with the open side [a one-way ANOVA]; n = 70 cells in each side of the OB from four individuals). Newborn GC dendrites had a lower spine density in the closed than the open side of the OB.

(legend continued on next page)

(*BDNF*) expression (Bloodgood et al., 2013; Lin et al., 2008; Ooe et al., 2004; Pruunsild et al., 2011; Ramamoorthi et al., 2011). A lentiviral system was used to provide either a gain or loss of function of *Npas4* in the OB interneurons during development, and *Npas4* knockout mice were used to show that Npas4 regulates dendritic spine development in OB GCs in a sensory-experience-dependent manner. Chromatin immunoprecipitation sequencing (ChIP-seq) and ISH analyses were performed to identify the novel target of Npas4, an E3 ubiquitin ligase *murine double minute 2* (*Mdm2*) gene, which was expressed at low levels in the wild-type OB but at higher levels in the *Npas4* knockout OB (Figure S1B). Finally, isobaric tags for relative and absolute quantitation (iTRAQ) and western blot (WB) analyses were performed to identify the novel target of Mdm2, a microtubule-associated protein doublecortin (Dcx), which was ubiquitinated and degraded via Mdm2 and resulted in a reduction in the dendritic spine density of the OB GCs (Figure S1C).

RESULTS

Npas4 Shows Sensory-Input-Dependent Expression in a Subset of Newborn OB Interneurons

To test whether sensory input affects the synapse development (synaptogenesis) of newborn mouse OB interneurons, a lentiviral vector expressing membrane-associated *GAP43-tagged enhanced yellow fluorescent protein* (*gapEYFP*) under the control of the *cytomegalovirus* promoter (*CMVp—gapEYFP*) was injected into the lateral ventricles (LVs) on postnatal day 0 (P0), followed by a unilateral naris occlusion. After 3 weeks (P21), we analyzed the synaptogenesis of newborn OB interneurons by confocal microscopy (Figure 1A). Measurement of the spine density of the GC dendrites (Figures 1B–1D) from P21 naris-occluded mice showed that there was a 1.3-fold reduction in the closed side compared to the open side of the OB (n = 70 cells; $p < 0.01$). These results confirm that odor-evoked sensory input is necessary for the dendritic spine development of OB GCs (Kelsch et al., 2009; Saghatelyan et al., 2005).

To investigate the molecules involved in regulating the development of OB interneurons, we searched for genes whose expression levels differed between the open and closed sides of the OB and whose expression correlated with the interneurons, based on DNA microarray plus ISH screenings (Yoshihara et al., 2012). In addition to the trophoblast glycoprotein *5T4* gene (Yoshihara et al., 2012), we found a transcription factor *Npas4* gene that shows clear differences in its expression between the open and closed sides of the OB (Figures 1E and 1F). Npas4 regulates the development of inhibitory synapses in excitatory neurons by regulating the expression of activity-dependent genes (Lin et al., 2008), suggesting that Npas4 could be a factor that regulates dendritic spine development and the synaptic connectivity of OB *Npas4*$^+$ neurons, depending on the degree of sensory input. Thus, we chose to examine the expression of *Npas4* in the OB, and following naris occlusion, in more detail. *Npas4* was expressed in a subset of GCs in the mitral cell and superficial GC layers (Figure 1E). In the olfactory-deprived side of the OB, *Npas4*$^+$ cell numbers decreased 1.7-fold in the mitral cell and superficial GC layers (n = 10 sections; $p < 0.01$; Figures 1E and 1F). Moreover, the average *Npas4* fluorescence hybridization signals decreased 1.9-fold in the closed side of the OB compared with those in the open side (n = 10 sections; $p < 0.01$; Figures 1E and 1F). By contrast, olfactory stimulation with a high concentration of the odorant amyl acetate immediately induced *Npas4* expression in the OB (n = 10 sections; $p < 0.01$; Figures 1G and 1H), as previously described (Bepari et al., 2012a). As shown in Figures 1I and 1J, in the GC layer, 97% of *Npas4*$^+$ cells expressed *GAD67* (GABAgenic neuronal marker), whereas 30% of *GAD67*$^+$ cells expressed *Npas4* (n = 6 sections). These results demonstrate that *Npas4* is expressed in a subset of GCs and that its expression depends on the level of sensory input.

Overexpression of *Npas4* Increases the Dendritic Spine Density of OB GCs

To investigate the role of Npas4 in neuronal development within the OB, a gain-of-function experiment was performed by injecting a lentiviral vector carrying the *CMVp—Npas4—internal ribosome entry site* (*IRES*)*—gapEYFP* construct into the LVs of P0 mice. After 2 weeks (P14), the synaptogenesis of the *Npas4*-expressing neurons was compared with that of the control *mCherry*-expressing neurons. The differences in the dendritic spine density between the control and *Npas4*-overexpressing GCs were dependent on the distance from the cell body (Figures 2A and 2B). For example, the spine density in the distal region of the GC dendrites, defined as the region from the dendritic tip to the branching point, increased 1.4-fold in *Npas4*-overexpressing GCs compared with that of the control mCherry$^+$ GCs (n = 20

(E) Fluorescence ISH of OB sections from P21 naris-occluded mice. *Npas4* hybridization and DAPI signals are shown in red and blue, respectively. *Npas4*$^+$ GCs, which were less numerous in the closed than in the open side of the OB, were located mainly in the mitral cell layer (MCL) and superficial GC layer (GCL). The scale bar represents 30 μm.

(F) Cell numbers (left) and hybridization-signal intensities (right) of the *Npas4*$^+$ GCs are shown as the mean ± SEM (left: open = 63 ± 6 cells/0.01 mm^2, closed = 37 ± 4 cells/0.01 mm^2; right: open = 100% ± 8%, closed = 52% ± 6%; **$p < 0.01$ compared with the open side [a one-way ANOVA]; n = 10 sections in each side of the OB from three individuals).

(G) Fluorescence ISH of OB sections from P21 odor-stimulated mice. Stimulation with the odorant amyl acetate led to immediate induction of *Npas4* expression in the OB. The scale bar represents 30 μm.

(H) Cell numbers (left) and hybridization-signal intensities (right) of the *Npas4*$^+$ GCs are expressed as the mean ± SEM (left: pretreatment = 13 ± 2 cells/0.01 mm^2, odor stimulation = 92 ± 4 cells/0.01 mm^2; right: pretreatment = 100% ± 6%, odor stimulation = 242% ± 4%; **$p < 0.01$ compared with the pretreatment condition [a one-way ANOVA]; n = 10 sections per bar from three individuals).

(I) Double ISH with the *Npas4* (magenta) and *GAD67* (GABAgenic neuronal marker, green) probes in OB sections from P21 odor-stimulated mice. The scale bar represents 30 μm.

(J) Ratios of *Npas4*$^+$ *GAD67*$^+$ GCs to *Npas4*$^+$ GCs (left) and *Npas4*$^+$ *GAD67*$^+$ GCs to *GAD67*$^+$ GCs (right) in the OBs of P21 odor-stimulated mice are shown as the mean ± SEM (left: 97% ± 1%; right: 30% ± 3%; n = 6 sections from each side of the OB from three individuals).

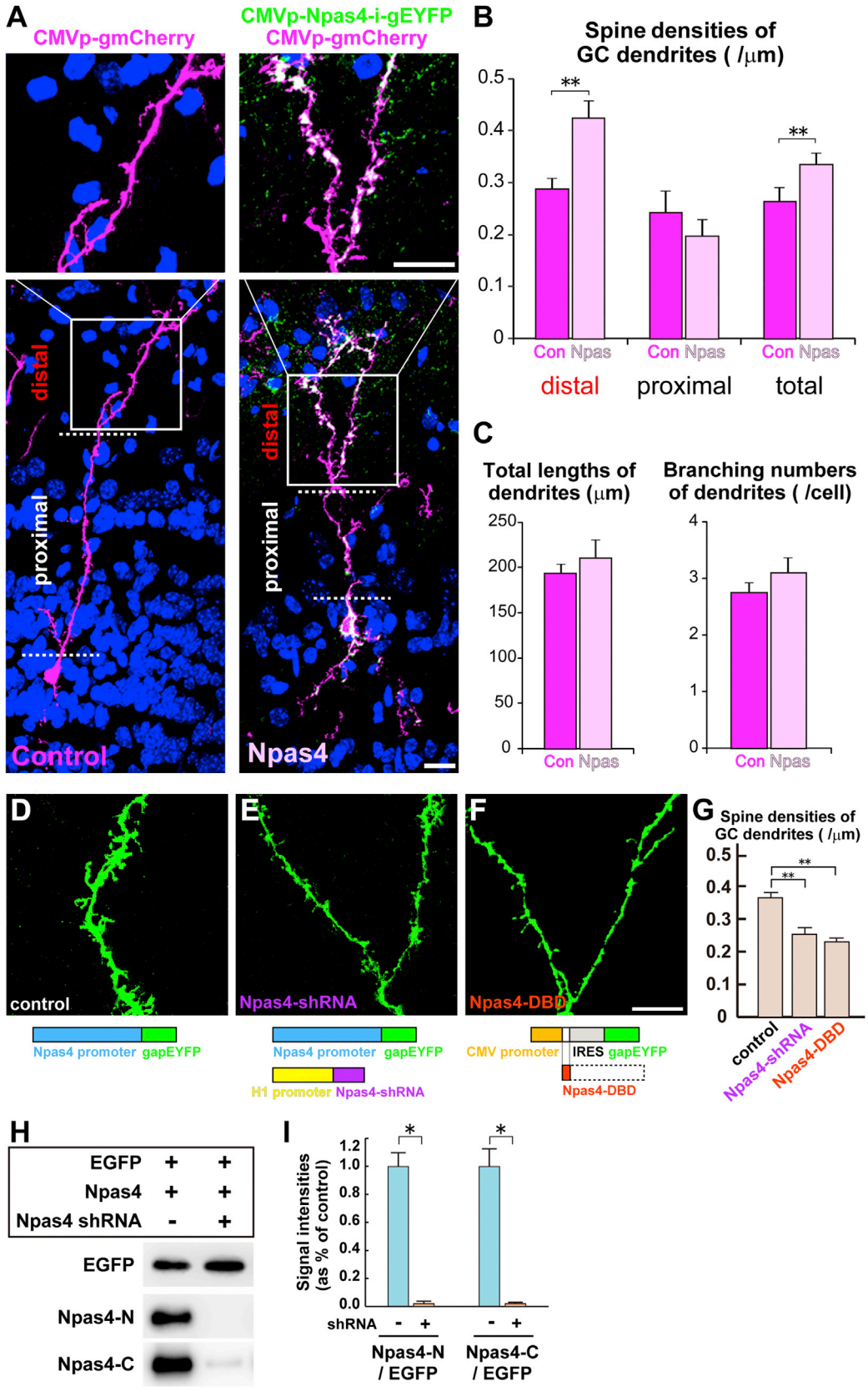

(legend on next page)

cells; $p < 0.01$; Figures 2A and 2B). However, in the proximal region, defined as the region from the branching point to the cell body, there was no difference in the spine density between the *Npas4*-overexpressing GCs and control GCs (n = 20 cells; Figures 2A and 2B). Therefore, in all subsequent experiments, the spine density of the GC dendrites was measured in the distal region. Notably, a similar dendritic domain-specific spine formation regulated by the *Npas4* gene was reported in the hippocampal Cornu Ammonis area 1 pyramidal neurons (Bloodgood et al., 2013).

Npas4 overexpression in newborn GCs at the adult stage, following infection of P56 mice, yielded results (a 1.3-fold increase in the spine density) similar to those seen in the neonatal animals (n = 20 cells; $p < 0.01$; Figures 2A, 2B, and S2A). Furthermore, *Npas4* overexpression increased the number of puncta in the distal region of the GC dendrites that were stained by either postsynaptic (postsynaptic density protein 95 [PSD-95] or gephyrin) or presynaptic (synaptoporin) markers (n = 20 cells; $p < 0.01$; Figure S3). These results demonstrate that *Npas4* overexpression facilitates both presynaptic and postsynaptic development in the distal region of the GC dendrites in the OB. *Npas4* overexpression produced no significant differences in either the total length or the branching number of GC dendrites (n = 20 cells; Figure 2C).

As shown above, olfactory sensory deprivation reduced the spine density of the GC dendrites (Figures 1B–1D). To test whether the dendritic spine density could be increased by *Npas4* overexpression under these conditions of reduced activity, two lentiviral vectors, *CMVp—Npas4—IRES—gapEYFP* and control *CMVp—gapmCherry*, were coinjected into the LVs of P0 mice, followed by a unilateral naris occlusion (Figures S2B and S2C). As expected, after 2 weeks (P14), GCs expressing the control *mCherry* had 1.2-fold fewer spines in the closed than in the open side of the OB (n = 20 cells; $p < 0.01$; Figures S2B and S2C). Interestingly, *Npas4*-overexpressing GCs possessed 1.3- and 1.5-fold more spines in the open and closed sides of the OB, respectively (n = 20 cells; $p < 0.01$; compared to the controls; Figures S2B and S2C). These results demonstrate that *Npas4* overexpression augments the dendritic spine density of the OB GCs and prevents the occlusion-induced reduction of the spine density.

Npas4 Loss of Function Leads to a Reduction in the Dendritic Spine Density of OB GCs

To further investigate the influence of *Npas4* in the development of *Npas4*$^{+}$ GCs, knockdown or dominant-negative lentiviral vectors were used in conjunction with an *Npas4* promoter construct to identify the interneurons with endogenous *Npas4* expression. To evaluate the *Npas4* promoter, which contains a 7 kb region upstream of the initiation codon, we injected the *Npas4* promoter-driven *gapmCherry* (*Npas4p—gapmCherry*) vector into the LVs of P3 *Npas4*$^{+/-}$ mice in which the *Npas4* coding region had been replaced by *green fluorescent protein* (*GFP*) (Lin et al., 2008) and performed immunostaining with antibodies against mCherry and GFP at P16. This revealed a subset of GCs, particularly in the mitral cell and superficial GC layers (in which mCherry^{+} GCs coexpressed the *GFP* gene), corresponding to the endogenous *Npas4* (Figure S4A). Therefore, in the following experiments, we analyzed the dendritic morphology of *Npas4p—gapEYFP*-expressing GCs, corresponding to the endogenous *Npas4*$^{+}$ GCs.

In the *Npas4* knockdown studies, we used lentiviral vectors that express *Npas4-short hairpin RNA* (*Npas4-shRNA*) under the human *H1* promoter (*H1p—Npas4-shRNA*). Both the *H1p—Npas4-shRNA* and *Npas4p—gapEYFP* vectors were coinjected into the LVs of P0 mice. Interestingly, coexpression of the *Npas4-shRNA* and *EYFP* constructs resulted in a 1.4-fold lower spine density of the GC dendrites than in the control *Npas4p—gapEYFP* dendrites (n = 20 cells; $p < 0.01$; Figures 2D, 2E, and 2G). This result shows that the *Npas4* knockdown leads to a reduction in the spine density of the GC dendrites. Notably, Npas4 protein and mRNA were efficiently decreased

Figure 2. *Npas4* Overexpression and Knockdown Facilitates and Represses the Development of Dendritic Spines in Newborn OB GCs, Respectively

(A) A lentiviral vector carrying the control construct (*CMVp—gmCherry*) was injected into the LVs of P0 mice, either alone or together with a second vector carrying the *Npas4* construct (*CMVp—Npas4—i—gEYFP*). mCherry^{+} GCs (magenta) and EYFP^{+} mCherry^{+} GCs (white) were analyzed 2 weeks (P14) after injection. We defined the proximal region as that from the soma to the first branching point of the apical dendrites and the distal region as that from the branching point to the dendritic tip. The scale bar represents 25 μm.

(B) The spine density of the GC dendrites is expressed as the mean ± SEM (distal: control = 0.29 ± 0.02/μm, Npas4 = 0.42 ± 0.03/μm; proximal: control = 0.24 ± 0.04/μm, Npas4 = 0.20 ± 0.03/μm; total: control = 0.26 ± 0.03/μm, Npas4 = 0.33 ± 0.02/μm; **$p < 0.01$ compared with the control [a one-way ANOVA]; n = 20 cells per line from three individuals). *Npas4* overexpression increased the spine density in the distal regions of the GC dendrites compared with that of the controls.

(C) The total lengths (left) and branching numbers (right) of the GC dendrites are expressed as the mean ± SEM (left: control = 193 ± 11 μm, Npas4 = 210 ± 20 μm; right: control = 2.8 ± 0.2/cell, Npas4 = 3.1 ± 0.3/cell).

(D and E) The *Npas4* knockdown experiment. A lentiviral vector carrying the control construct (*Npas4p—gapEYFP*) was injected either alone (D) or together with *Npas4 shRNA* (*H1p—Npas4-shRNA*) (E) into the LVs of P0 mice. Coexpression of the *Npas4-shRNA* and *EYFP* constructs (E) gave rise to a lower spine density of the GC dendrites than expression of the control vector alone (D).

(F) The *Npas4* dominant-negative experiment. Expression of the *CMVp—Npas4-DNA binding domain* (*DBD*)*—IRES—gapEYFP* vector (F) gave rise to a reduction in the spine density of the GCs when compared with expression of the control construct (D). The scale bar represents 10 μm.

(G) The spine density (D–F) of the GC dendrites is expressed as the mean ± SEM (control = 0.36 ± 0.01/μm, Npas4 shRNA = 0.25 ± 0.02/μm, Npas4 DBD = 0.23 ± 0.01/μm; **$p < 0.01$ compared with the control [a one-way ANOVA]; n = 20 cells per line from three individuals).

(H) The efficiency of *Npas4* knockdown. WB analysis of HEK293T cell lysates cotransfected with *CMVp—enhanced GFP* (*EGFP*) and *CMVp—Npas4* with or without *H1p—Npas4-shRNA*. Npas4 protein was detected using two antibodies (Npas4-N and Npas4-C).

(I) The intensities of individual bands in (H) were normalized against that of enhanced GFP (EGFP) and are expressed as the mean ± SEM (Npas4-N/EGFP: control = 1.0 ± 0.01, Npas4 shRNA = 0.02 ± 0.01; Npas4-C/EGFP: control = 1.0 ± 0.12, Npas4 shRNA = 0.02 ± 0.01; *$p < 0.05$ compared with control values [a one-way ANOVA]).

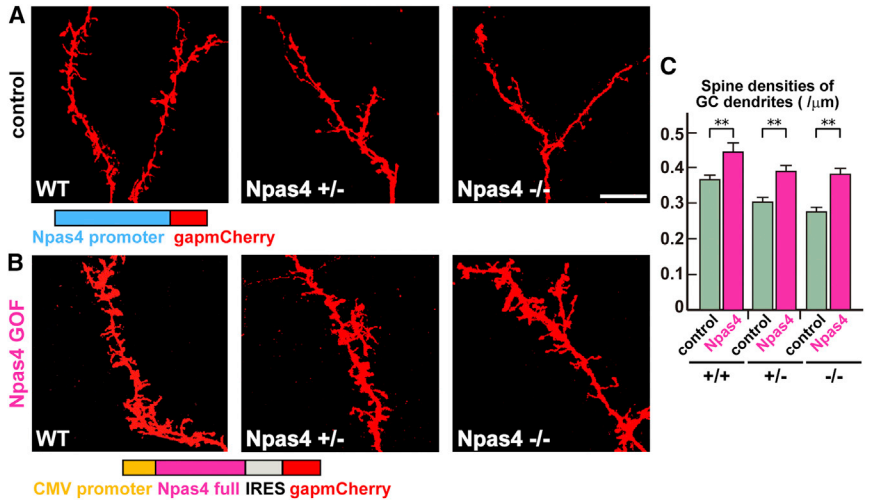

Figure 3. Expression of *Npas4* Rescues the Reduction in the Dendritic Spine Density of the OB GCs from *Npas4* Knockout Mice

(A) *Npas4* knockout mice. A lentiviral vector carrying *Npas4p—gapmCherry* was injected into the LVs of *Npas4*$^{+/+}$, *Npas4*$^{+/-}$, and *Npas4*$^{-/-}$ mice at P3, and OB sections were immunostained with an mCherry antibody at P17. *Npas4* gene dosage appears to correlate with the degree of the dendritic spine development. The scale bar represents 10 μm. WT, wild-type.

(B) *Npas4* gain of function (GOF) in *Npas4* knockout mice. Overexpression of *Npas4* by a lentiviral vector carrying *CMVp—Npas4—IRES—gapmCherry* rescued the reduction in the dendritic spine density seen in *Npas4* mutant GCs.

(C) The spine density (A and B) of the GC dendrites is expressed as the mean ± SEM (*Npas4*$^{+/+}$: control = 0.36 ± 0.01/μm, Npas4 GOF = 0.44 ± 0.03/μm; *Npas4*$^{+/-}$: control = 0.30 ± 0.01/μm, Npas4 GOF = 0.39 ± 0.02/μm; *Npas4*$^{-/-}$: control = 0.28 ± 0.01/μm, Npas4 GOF = 0.38 ± 0.02/μm; **p < 0.01 compared with the control [a one-way ANOVA]; n = 20 cells per line from three individuals).

by *Npas4-shRNA*, respectively, both in vitro and in vivo (Figures 2H, 2I, and S4B).

Next, we hypothesized that the overexpression of the Npas4-DNA binding domain (DBD) alone might inhibit DNA binding of the endogenous Npas4 and therefore affect the spine development of the GC dendrites. Consistent with this, injection of a lentiviral vector carrying the *CMVp—Npas4-DBD—IRES—gapEYFP* construct into the LVs resulted in a reduction in the spine density of the GC dendrites compared with that of mice infected by the control *CMVp—gapEYFP* vector (n = 20 cells; p < 0.01; Figures 2D, 2F, and 2G). This supports the possibility that the *Npas4-DBD* acts in a dominant-negative manner. Thus, two different types of experiments demonstrate that *Npas4* loss of function reduces the dendritic spine density in the OB GCs.

Expression of *Npas4* Rescues the Reduction in the Dendritic Spine Density of OB GCs from *Npas4* Knockout Mice

To further explore the effects of *Npas4* loss of function in the OB interneurons, we analyzed *Npas4*$^{+}$ GCs in *Npas4* knockout mice in which the *Npas4* coding region was replaced by *GFP* (Lin et al., 2008). We then injected a lentiviral vector carrying the *Npas4* promoter-driven *gapmCherry* (*Npas4p—gapmCherry*) into the LVs of *Npas4*$^{+/+}$, *Npas4*$^{+/-}$, and *Npas4*$^{-/-}$ mice at P3 and immunostained OB sections with an mCherry antibody at P17. The dendrites of mCherry^{+} (endogenous *Npas4*$^{+}$) GCs in the heterozygotes showed a spine density 1.2-fold lower than that of the wild-type mice (n = 20 cells; p < 0.01; Figures 3A and 3C), whereas the dendrites of null mice showed a spine density 1.3-fold lower than that of the wild-type mice (n = 20 cells; p < 0.01; Figures 3A and 3C). Thus, the *Npas4* gene dosage correlates with the degree of the dendritic spine development. Remarkably, the reduction in the dendritic spine density of the *Npas4* mutant GCs could be rescued by the overexpression of *Npas4* with a lentiviral vector carrying the *CMVp—Npas4—IRES—gapmCherry* construct (n = 20 cells; p < 0.01; Figures 3A–3C).

Then, we examined the effect of sensory input on the dendritic spine density of mCherry^{+} GCs in *Npas4* mutant mice. In the wild-type mice, the spine density of mCherry^{+} GCs was reduced 1.3-fold under naris-occluded conditions (n = 20 cells; p < 0.01; Figures S5A–S5C), which is consistent with Figure 1. By contrast, the spine density of GC dendrites in the *Npas4*-null mice did not differ between the open and closed sides of the OB (n = 20 cells; Figures S5A–S5C). These results strongly suggest that Npas4 is both necessary and sufficient for regulating sensory-input-dependent synaptogenesis in the OB GCs.

Loss of *Npas4* Upregulates *Mdm2* Expression to Reduce the Dendritic Spine Density of OB GCs

Although Npas4 induces the expression of *BDNF* and *c-fos* in hippocampal neurons (Bloodgood et al., 2013; Lin et al., 2008; Ramamoorthi et al., 2011), the *BDNF* and *c-fos* expression did not differ between the wild-type and *Npas4*-null OBs (Figures S6A and S6B). This result suggests that Npas4 may induce the expression of other target genes in the OB GCs to facilitate dendritic spine formation. To identify the target genes through which Npas4 regulates synaptogenesis in the OB interneurons, we performed ChIP-seq analysis in homogenized OB tissues using two different antibodies against Npas4. As shown in Table S1, ChIP-seq produced many hits with both Npas4 antibodies, perhaps because Npas4 binds to an E-box-like DNA sequence, CA(C/G)(G/C)TG, which is GC-rich (Ooe et al., 2004). We then searched the ChIP-seq-derived genes to identify those with expression levels that differed between the OBs of the wild-type and *Npas4*-null mice and whose expression was detected in the interneurons, as assessed by ISH. Among ~100 genes, we identified the target of Npas4, an oncogenic ubiquitin ligase *Mdm2* gene, showing a clear difference in expression between the wild-type and *Npas4* knockout OBs (Figure 4A). In addition, *Mdm2* expression was clearly increased in GCs in which

Npas4 had been knocked down by *Npas4-shRNA* (Figure S4C). Like *Mdm2*, the genes *Nedd4L* and *Ube2e3*, which also encode ubiquitin ligases in the ChIP-seq-derived genes (Table S1), were expressed more strongly in the *Npas4* knockout OB than the wild-type OB (Figure 4A). Notably, these genes were precipitated with the Npas4 antibody in the ChIP-PCR analysis (Figure 4B). These results suggested that *Mdm2*, *Nedd4L*, and *Ube2e3* seemed to be the novel target genes of Npas4.

Next, we performed a gain-of-function experiment by injecting a lentiviral vector containing the *CMVp—Mdm2—IRES—gapEYFP* construct into the LVs of wild-type P0 mice. This showed that overexpression of *Mdm2* reduced the spine density of the GC dendrites compared with a control *CMVp—gapEYFP* construct or with the overexpression of *Nedd4L* and *Ube2e3* ($n = 20$ cells; $p < 0.01$; Figures 4C and 4E). Furthermore, we performed a knockdown experiment by coinjecting two lentiviral vectors that express *H1p—Mdm2-shRNA* and *CMVp—gapEYFP* into the LVs of P0 mice. Interestingly, coexpression of the *Mdm2-shRNA* and *EYFP* constructs resulted in a 1.4-fold higher spine density of the GC dendrites than in the control *CMVp—gapEYFP* dendrites ($n = 20$ cells; $p < 0.01$; Figures 4C–4E). In the *CMVp—Npas4—IRES—gapEYFP* lentivirus-infected mice, *Mdm2* expression was lower in *Npas4*-overexpressing GFP^+ GCs than in GFP^- GCs (Figure 4F). This demonstrates that the knockdown of *Mdm2* enhances the spine density of the OB GC dendrites and that *Mdm2* is a bona fide target gene of Npas4.

Mdm2 Ubiquitinates and Degrades Dcx to Reduce the Dendritic Spine Density of OB GCs

Mdm2 E3 ligase is known to be localized at synapses and to ubiquitinate and degrade PSD-95 in rat hippocampal neurons (Colledge et al., 2003). However, no differences were detected in the amount of PSD-95 protein between the wild-type and *Npas4* knockout OBs by WB analysis (Figures 5A and 5B). To identify the protein targets through which Mdm2 regulates synaptogenesis in the OB interneurons, we performed iTRAQ protein analysis on four different OB tissue samples from two wild-type and two *Npas4* knockout mice. The iTRAQ analysis produced many hits, with a higher amount of protein in the wild-type OBs than in the *Npas4* knockout OBs (Table S2). Based on WB analyses of 17 candidates, we identified a target for Mdm2, the microtubule-associated protein Dcx, showing a clear difference in the amount of protein between the wild-type and *Npas4* knockout OBs (Table S2; Figures 5A and 5B). This was confirmed by immunohistochemistry (IHC) with the Dcx antibody to OB sections; Dcx fluorescence signals in the GC dendrites within both the external proximal layer (EPL) and the GC layer (GCL) were 2-fold higher in the wild-type OB than in the *Npas4* knockout OB (Figure 6A). The amount of Dcx protein was remarkably decreased in GCs, in which *Npas4* had been knocked down by *Npas4-shRNA* (Figure S4D). Similarly, Dcx-immunoreactive signals were decreased significantly in newborn bromodeoxyuridine $(BrdU)^+$ GCs from $Npas4^{-/-}$ mice compared to those from $Npas4^{+/+}$ mice (Figure 6C). There was a slight reduction in the Dcx signal intensity in the *Npas4* knockout RMS compared to the wild-type RMS (Figure 6B).

To examine whether Mdm2 would associate with Dcx for ubiquitination, we cotransfected three *CAG* promoter (*CAGp*)-driven plasmids, *CAGp—Dcx*, *CAGp—Mdm2*, and *CAGp—mCherry* (control), into a human embryonic kidney 293T (HEK293T) cell line, followed by immunoprecipitation (IP) and WB analyses. In the WB analysis, the Dcx band intensity decreased in the cotransfection with the *Dcx* and *Mdm2* plasmids, compared with the transfection with the *Dcx* plasmid (Figure 5C). This demonstrates that Mdm2 reduces the amount of Dcx protein. IP with the Dcx antibody and WB with the Mdm2 antibody showed a strong Mdm2 band only in the cotransfection with the *Dcx* and *Mdm2* plasmids, whereas IP with the Mdm2 antibody and WB with the Dcx antibody indicated a weak Dcx band only in the cotransfection with the *Dcx* and *Mdm2* plasmids (Figure 5D). This suggests that Mdm2 associates with Dcx for ubiquitination. Then, to examine whether Mdm2 would ubiquitinate Dcx, we cotransfected four plasmids carrying *CAGp—Dcx*, *CAGp—Mdm2*, *CAGp—hemagglutinin-ubiquitin* (*HA-Ub*), and *CAGp—mCherry* (control) into HEK293T cells, followed by IP with the Dcx antibody and WB with the HA antibody to detect ubiquitination (Figure 5E). Band shifts corresponding to polyubiquitinated Dcx were detected only in the cotransfection with the *Dcx* and *Mdm2* plasmids. This indicates that Mdm2 ubiquitinates Dcx for degradation. We further confirmed that *Dcx* was expressed in most $Npas4^+$ GCs at P7, whereas 51% of $Npas4^+$ GCs were Dcx^+ at P56 (Figure S7A), suggesting that *Npas4* is expressed in younger Dcx^+ and older Dcx^- GCs in adults.

Finally, we performed a gain-of-function experiment by injecting a lentiviral vector containing the *CMVp—Dcx—IRES—gapEYFP* construct into the OBs of wild-type P0 mice. We injected the lentiviral vector into the OB to overexpress Dcx specifically in OB neurons because Dcx also regulates OB neuroblast migration in the RMS (Belvindrah et al., 2011). This indicated that overexpression of *Dcx* enhanced the spine density of the GC dendrites, compared with a control *CMVp—gapEYFP* construct ($n = 20$ cells; $p < 0.01$; Figure 6D). Furthermore, we performed a knockdown experiment by coinjecting two lentiviral vectors that express *H1p—Dcx-shRNA* and *CMVp—gapEYFP* into the OBs of P0 mice. Coexpression of the *Dcx-shRNA* and *EYFP* constructs resulted in a 1.4-fold lower spine density of the GC dendrites than in the control *CMVp—gapEYFP* dendrites ($n = 20$ cells; $p < 0.01$; Figure 6D). This indicates that the *Dcx* knockdown reduces the spine density of the OB GC dendrites like the *Npas4* knockout does (Figure 3). In addition, we measured both the total length and branching number of dendrites in control, *Dcx*-overexpressing, and *Dcx* knockdown GCs, located in the superficial GCL. There was no difference in either the total length or branching number of GC dendrites (Figure 6D), like *Npas4* gain or loss of function (Figures 2A–2C; S.Y., unpublished data). These results reveal that Dcx plays an important role in regulating the dendritic spine density of the OB GCs, but not the dendritic length or branching number. Notably, *Dcx* was strongly expressed in younger mice OB at P7 but decreased in older mice OB at P56 (Figure S7A). Dcx protein was not detected in most of the 8-week-old GCs, labeled with the lentiviral vector carrying *CMVp—gapEYFP* at P0 (Figure S7B). Consistent with this observation, *Npas4* overexpression and knockdown did not affect the dendritic spine density in 8-week-old GCs (Figures S7C and S7D). In contrast, *Npas4* overexpression enhanced dendritic spine development in GCs, which were newly generated around

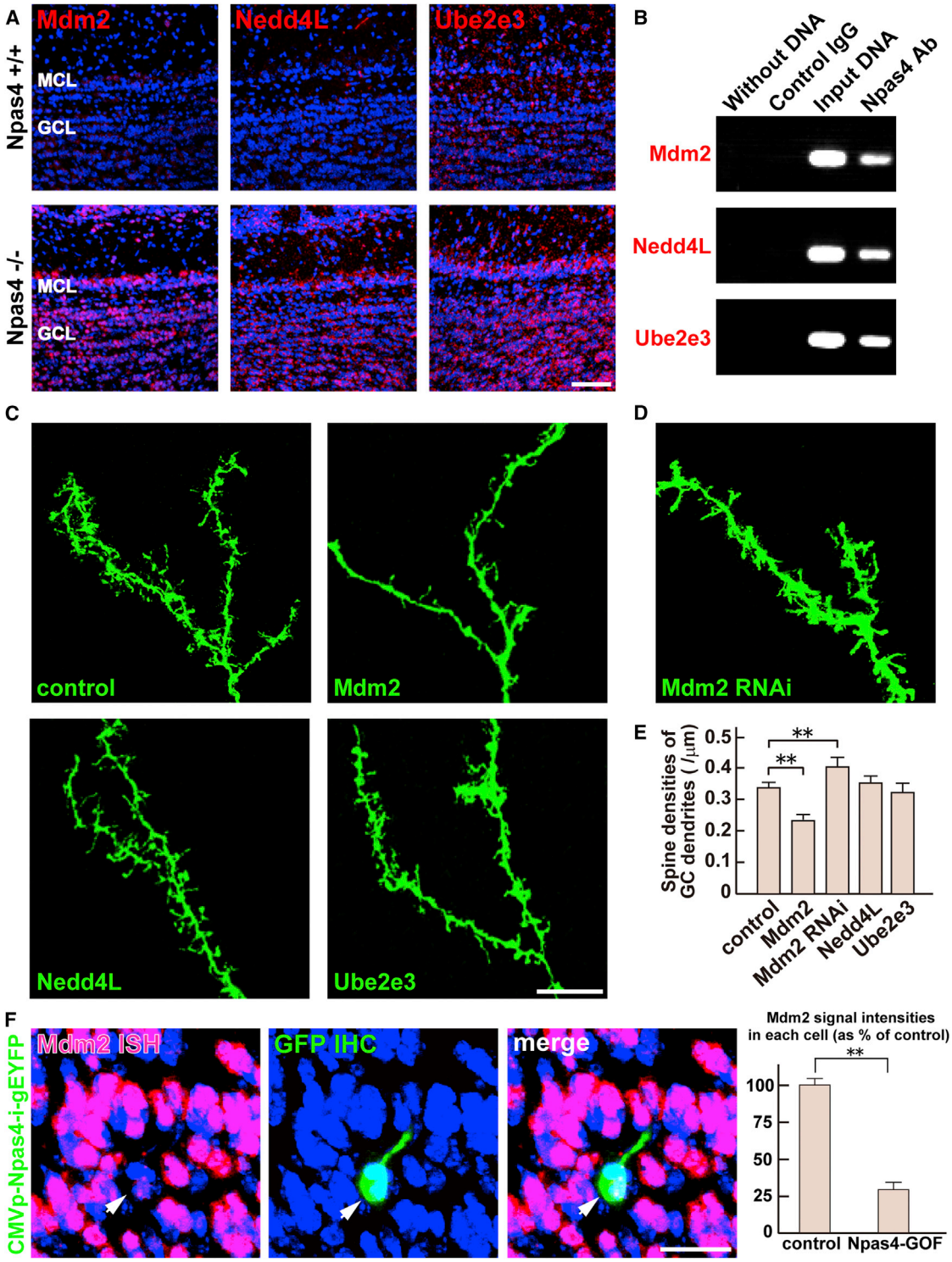

Figure 4. Loss of *Npas4* Upregulates *Mdm2* Expression, Leading to a Reduction in the Dendritic Spine Density of the OB GCs

(A) Fluorescence ISH of OB sections from *Npas4*$^{+/+}$ and *Npas4*$^{-/-}$ mice at P21. *Mdm2* expression was increased in the *Npas4* knockout OB compared with the wild-type OB. The same was true for *Ube2e3* and *Nedd4L*. The scale bar represents 60 μm.

(B) ChIP-PCR analysis. The upstream regions of *Mdm2*, *Ube2e3*, and *Nedd4L* genes were ChIP analyzed with an Npas4 antibody and amplified using specific sets of primers.

(legend continued on next page)

P56 (Figure S2A). Collectively, these results suggest that Npas4 regulates dendritic spine formation in newborn young Dcx$^+$ GCs, but not in older Dcx$^-$ GCs (Figure S7E).

Npas4 Loss of Function Specific to OB Neurons Impairs Odor Discrimination Learning

We examined whether spine formation in OB GCs is required for odor discrimination learning and memory in mice. Although global *Npas4* knockout mice have defects in the OB and in other brain regions (Lin et al., 2008), we generated OB-specific *Npas4* knockout mice by injecting a *Cre*-expression lentivirus (*CMVp—Cre—IRES—gapEYFP* gene) into both the LVs and OBs of *Npas4*$^{flx/flx}$ mice (Lin et al., 2008) at P3. The *Cre*-expression lentivirus was thereby infected into neural stem cells in the LVs as well as into OB cells, such as projection neurons and interneurons. However, as *Npas4* expression was restricted predominantly to *GAD67*$^+$ interneurons in the OB (Figures 1I and 1J), the effect of *Npas4* knockout was defined to OB interneurons. This resulted in OB interneuron-specific loss of *Npas4* expression in the *Npas4*$^{flx/flx}$ mice (~40% of the total GCs were Cre$^+$ Npas4$^-$; S.Y., unpublished data). After 6 weeks (P45), we conducted a test of odor discrimination learning and compared the performance of these mice with that of wild-type animals (Figure 7A; Imayoshi et al., 2008). Mice were trained for 4 days to associate an odor ((+) carvone) with a sugar reward. During the training, conditional *Npas4* knockout mice showed the sugar reward at the similar level to the wild-type mice. On day 5, we placed this odor ((+) carvone) and a related enantiomer ((–) carvone) separately underneath the bedding, without any sugar, and measured the time when the mice spent digging near each odor. Wild-type mice spent significantly more time near (+) carvone, which was associated with sugar ($n = 4$ individuals; $p < 0.05$; Figure 7B). However, OB-specific *Npas4* knockout mice divided their time equally between the two odors ($n = 4$ individuals; Figure 7B). Notably, olfactory detection ability of OB-specific *Npas4* knockout mice appeared to be similar to that of the wild-type mice in a food-finding test (S.Y., unpublished data). Because the *Cre*-expression lentiviral vector was injected into neural stem cells in the LVs of *Npas4*$^{flx/flx}$ mice at P3, *Npas4* gene was lost in older GCs as well as in younger GCs from the 6-week-old mice. These results indicate that loss of *Npas4* in young and old GCs impairs the acquisition of the two-related-odors discrimination task, but not the olfactory detection ability. This suggests that spine formation in interneuronal dendrites in the OB neural circuitry is required for odor-associated learning and memory.

DISCUSSION

Our ISH screen identified Npas4 as a candidate for promoting synaptogenesis in the distal portion of GC dendrites and revealed that its expression depends on the degree of sensory input. *Npas4* is expressed in OB GCs immediately after sensory input and is required for dendritic spine formation. *Npas4* overexpression in newborn interneurons increased the spine densities of the GC dendrites, even under sensory deprivation, and rescued the reduction in the spine density of the GC dendrites from *Npas4* knockout OB. Furthermore, the loss of *Npas4* upregulated the expression of *Mdm2* to increase the ubiquitination and degradation of Dcx and led to a reduction in the dendritic spine density of the OB GCs.

How Can Sensory Experience Influence *Npas4* Expression in OB GCs?

Sensory experience has long been recognized as being important in shaping development and plasticity throughout the nervous system (Katz and Shatz, 1996; Nithianantharajah and Hannan, 2006; Sanes and Lichtman, 2001). Specific odorants activate olfactory sensory neurons (OSNs) that express corresponding odorant receptors. OSNs project to specific glomeruli in the OB and can subsequently activate a specific OB neural circuit locally, upregulating the expression of *5T4* in GCs and PGCs via mitral and tufted cells (Yoshihara et al., 2012). Our experiments reveal that the increased expression of *Npas4* facilitates spine development, but not arborization, in GC dendrites of the OB. The increased dendritic spine density of *Npas4*$^+$ GCs may make it possible to integrate inputs and outputs from a larger receptive field; this would be consistent with the immediate increase in *Npas4* expression in the OB associated with sensory stimulation (Bepari et al., 2012a). Thus, *Npas4*$^+$ interneurons that are connected to glomeruli directly or indirectly via other neurons such as mitral/tufted cells can be activated by specific odorants. It is possible that Npas4 plays an important role in regulating the activity-dependent synapse development in OB GCs.

Npas4 is a critical factor that regulates the inhibitory synapse development of excitatory neurons (Lin et al., 2008) and is involved in both learning and memory (Ploski et al., 2011; Yun et al., 2010). Although *Npas4* expression is selectively induced by membrane depolarization and Ca^{2+} influx, it is not induced by several neurotrophic factors, including BDNF and NT3, which readily induce other transcription factors such as c-fos and Arc (Bloodgood et al., 2013; Lin et al., 2008; Ramamoorthi et al.,

(C) The GOF experiment. A lentiviral vector carrying *CMVp—Mdm2* (*Nedd4L* or *Ube2e3*)*—IRES—gapEYFP* was injected into the LVs of wild-type P0 mice. Overexpression of *Mdm2* reduced the spine density of the GC dendrites compared with the control construct or with overexpression of *Nedd4L* or *Ube2e3*. The scale bar represents 10 μm.

(D) The knockdown experiment. Two lentiviral vectors carrying *H1p—Mdm2-shRNA* and *CMVp—gapEYFP* were coinjected into the LVs of wild-type P0 mice. The *Mdm2* knockdown enhanced the spine density of the OB GC dendrites. The scale bar represents 10 μm.

(E) The spine density (C and D) of the GC dendrites is expressed as the mean ± SEM (control = 0.32 ± 0.02/μm; Mdm2 = 0.22 ± 0.02/μm; Mdm2 RNAi = 0.40 ± 0.03/μm; Nedd4L = 0.34 ± 0.02/μm; Ube2e3 = 0.31 ± 0.03/μm; **$p < 0.01$ compared with the control [a one-way ANOVA]; $n = 20$ cells per line from three individuals).

(F) *Npas4* overexpression experiment. A lentiviral vector carrying the *Npas4*-overexpression construct (*CMVp—Npas4—i—gEYFP*) was injected into the LVs of P0 wild-type mice. GFP IHC and *Mdm2* ISH were performed in OB sections of these mice at P14. *Mdm2* expression was lower in *Npas4*-overexpressing GFP$^+$ GCs than in GFP$^-$ GCs (data expressed as the mean ± SEM; control = 100% ± 5%; *Npas4* overexpression = 35% ± 4%; $n = 20$ cells of the OB from three individuals). The scale bar represents 20 μm.

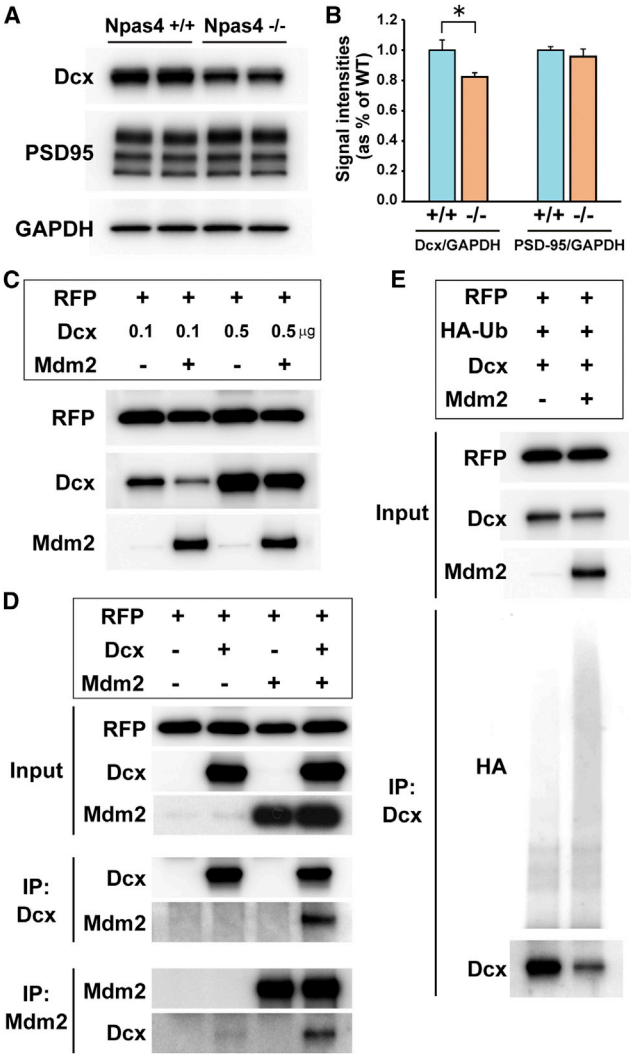

Figure 5. Mdm2 Ubiquitinates and Degrades Dcx to Reduce the Dendritic Spine Density in the OB GCs

(A) WB analysis of OB lysates from *Npas4*$^{+/+}$ and *Npas4*$^{-/-}$ mice at P21. The amount of Dcx protein decreased in the *Npas4* knockout OB compared with the wild-type OB.

(B) The intensities of each band were normalized to GAPDH and expressed as the mean ± SEM (Dcx/GAPDH: *Npas4*$^{+/+}$ = 100 ± 7, *Npas4*$^{-/-}$ = 82 ± 2; PSD-95/GAPDH: *Npas4*$^{+/+}$ = 100 ± 2, *Npas4*$^{-/-}$ = 96 ± 5; *p < 0.05 compared with wild-type values [a one-way ANOVA]; OB lysates were prepared from four individuals of each genotype).

(C and D) WB analysis of HEK293T cell lysates cotransfected with three plasmids: *CAGp—Dcx*, *CAGp—Mdm2*, and *CAGp—mCherry*. (C) Dcx band intensity decreased in the cotransfection with the *Dcx* and *Mdm2* plasmids (lanes 2 and 4), compared with the transfection with the *Dcx* plasmid (lanes 1 and 3). (D) Immunoprecipitation of Dcx and Mdm2. The Mdm2 and Dcx antibodies coprecipitated Mdm2 and Dcx, respectively.

(E) Ubiquitination of Dcx in HEK293T cell lysates cotransfected with four plasmids: *CAGp—Dcx*, *CAGp—Mdm2*, *CAGp—hemagglutinin-ubiquitin* (*HA-Ub*), and *CAGp—mCherry*. Cell lysates were immunoprecipitated with the Dcx antibody, followed by WB with the HA antibody, to detect ubiquitination.

2011). After contextual fear conditioning, *Npas4* induction occurs as early as 5 min after training, much earlier than *c-fos* induction (Ramamoorthi et al., 2011). This suggests that the pathways that induce *Npas4* expression could be different from those that induce other immediate-early genes (Bepari et al., 2012b). We recently found that the 7 kb *Npas4* promoter used in this study contains putative binding motifs for activity-dependent transcription factors such as *CREB*, *Sp1*, *egr1*, *GATA-1*, *AP-4*, *Oct-1*, *Npas4*, and other genes (S.Y., unpublished data). Further studies on the 7 kb promoter will enable us to elucidate the mechanisms by which *Npas4* gene expression is regulated on the basis of sensory input.

How Does Npas4 Regulate the Dendritic Synapse Development of OB GCs?

Our results revealed that Npas4 signaling is necessary and sufficient for regulating pre- and postsynaptic development of OB GCs on the basis of sensory experience. Moreover, ChIP-seq and ISH identified an E3 ubiquitin ligase *Mdm2* gene that showed clear differences in its expression between the wild-type and *Npas4* knockout OBs. Our results indicate that Npas4 downregulates the expression of *Mdm2*, *Nedd4L*, and *Ube2e3*. Although Npas4 acts as a transcriptional activator and can induce the expression of *BDNF* and *c-fos* in the hippocampus (Bloodgood et al., 2013; Lin et al., 2008; Pruunsild et al., 2011), it was recently reported that Npas4 represses the expression of a *mitochondrial calcium uniporter* (*Mcu*) gene in hippocampal neurons (Qiu et al., 2013). Taken together, we speculate that Npas4 can function as either a transcriptional activator or repressor, depending on the cell types and the downstream genes.

Mdm2 is localized at synapses and ubiquitinates and degrades the postsynaptic scaffold, PSD-95, in rat hippocampal neurons (Colledge et al., 2003). However, our iTRAQ and WB analyses identified, instead of PSD-95, a microtubule-associated protein Dcx that showed a clear difference in the amount of protein between the wild-type and *Npas4* knockout OBs. Despite the widespread use of Dcx as a marker for immature neurons in the adult neurogenic lineage (Brown et al., 2003), little is known about its specific function in adult neurogenesis, except that Dcx regulates the migration and dendritic development of migrating neurons in the OB core region, including the deep GCL and the RMS (Belvindrah et al., 2011). Our results reveal that *Dcx* overexpression and knockdown in the OB do not affect the dendritic length and branching number of GCs in the superficial GCL. Alternatively, we found that Dcx regulates the spine development of the OB GC dendrites in concert with Mdm2, for ubiquitination and degradation, based on the following evidence. First, IHC of OB sections showed that Dcx signals in GC dendrites within the EPL and the GCL were 2-fold higher in the wild-type OB than *Npas4* knockout OB. Second, IP and WB analyses indicated that Mdm2 is associated with Dcx for ubiquitination and degradation. Third, the overexpression of *Dcx* in OB GCs enhanced the dendritic spine density, whereas the knockdown of *Dcx* in OB GCs reduced the dendritic spine density. Taken together, these results reveal that *Npas4* downregulates *Mdm2* expression to reduce the ubiquitination and degradation of Dcx and leads to an increment in the

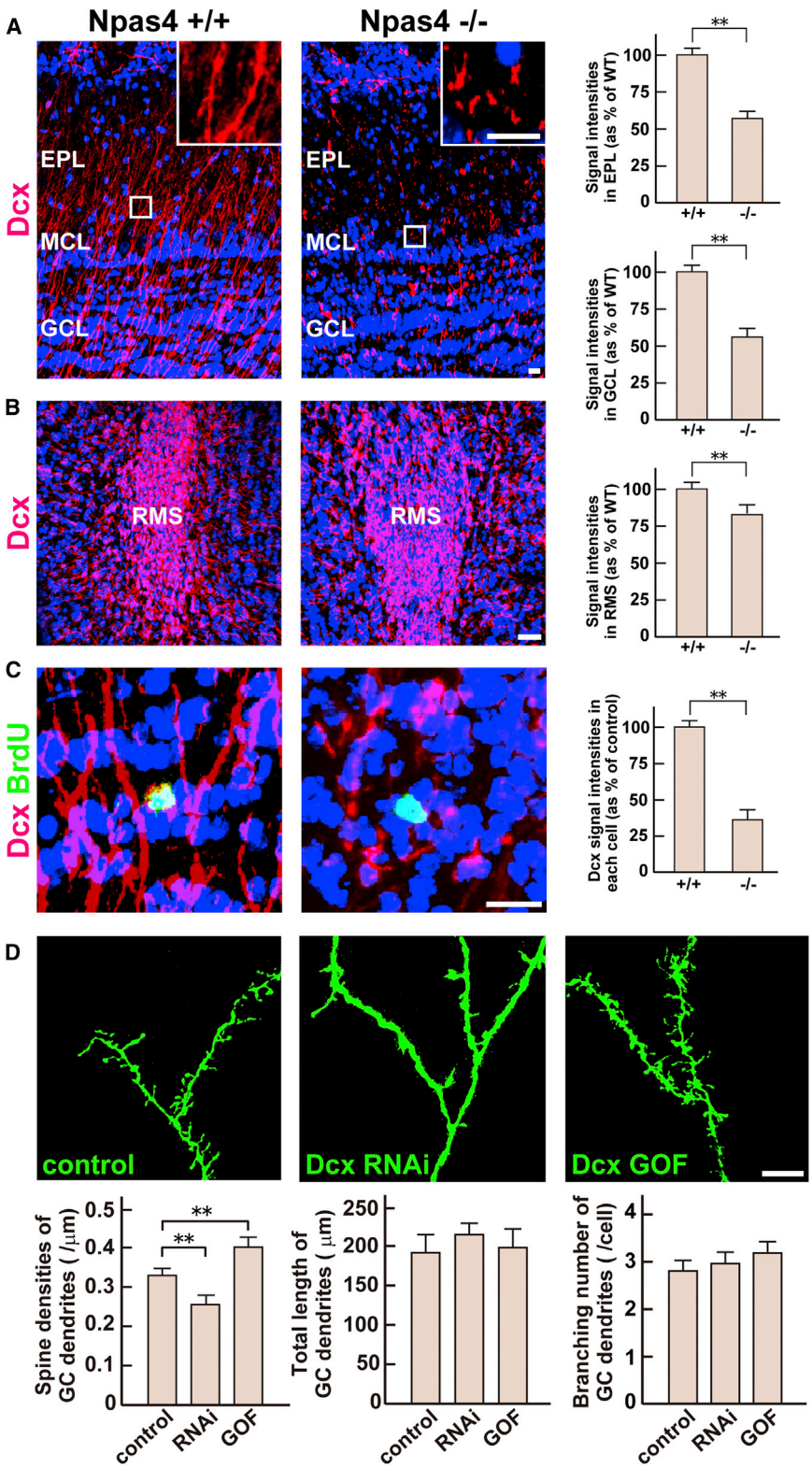

Figure 6. Dcx Regulates the Dendritic Spine Development of OB GCs

(A and B) Dcx IHC of OB sections from *Npas4*$^{+/+}$ and *Npas4*$^{-/-}$ mice at P21. The amount of Dcx protein was decreased in the EPL, GCL, and RMS of the *Npas4* knockout OB compared with those of the wild-type OB. Insets show enlarged images of the area enclosed by white squares. The scale bars represent 20 μm in (A) and 40 μm in (B). The Dcx signal intensity (A and B) is expressed as the mean ± SEM (EPL: *Npas4*$^{+/+}$ = 100% ± 6%, *Npas4*$^{-/-}$ = 56% ± 8%; GCL: *Npas4*$^{+/+}$ = 100% ± 5%, *Npas4*$^{-/-}$ = 52% ± 4%; RMS: *Npas4*$^{+/+}$ = 100% ± 5%, *Npas4*$^{-/-}$ = 81% ± 6%; **p < 0.01 compared with the *Npas4*$^{+/+}$ OBs [a one-way ANOVA]; n = 10 sections per line of the OB from three individuals).

(C) Dcx immunostaining of newborn young GCs in *Npas4*$^{+/+}$ and *Npas4*$^{-/-}$ OB. Newborn GCs were labeled by BrdU injection at P7 and subjected to BrdU immunostaining at P21. Dcx immunoreactive signals (red) were more decreased in newborn young BrdU^{+} GCs (green) of *Npas4*$^{-/-}$ mice than in those of *Npas4*$^{+/+}$ mice (data expressed as the mean ± SEM; *Npas4*$^{+/+}$ = 100% ± 6%, *Npas4*$^{-/-}$ = 34% ± 12%; **p < 0.01 compared with the *Npas4*$^{+/+}$ OBs [a one-way ANOVA]; n = 20 cells in each line from three individuals). The scale bar represents 20 μm.

(D) *Dcx* GOF and knockdown experiments. For the *Dcx* GOF, a lentiviral vector carrying *CMVp—Dcx—IRES—gapEYFP* was injected into OBs of wild-type P0 mice, leading to enhancement in the spine density of GC dendrites. For the *Dcx* knockdown (*Dcx* RNAi), two lentiviral vectors carrying *H1p—Dcx-shRNA* and *CMVp—gapEYFP* were coinjected into OBs of wild-type P0 mice, leading to reduction in the spine density of OB GC dendrites. The *Dcx* knockdown gave a 1.4-fold lower spine density of GC dendrites than the control (left graph). The scale bar represents 10 μm. The spine density of GC dendrites is expressed as the mean ± SEM (left graph: control = 0.32 ± 0.02/μm, Dcx RNAi = 0.25 ± 0.03/μm, Dcx GOF = 0.40 ± 0.03/μm; **p < 0.01 compared with the control [a one-way ANOVA]; n = 20 cells per line from three individuals). The total length (middle graph) and branching number (right graph) of dendrites in control, *Dcx* GOF, and *Dcx* RNAi GCs are expressed as the mean ± SEM (middle graph: control = 184 ± 22 μm, Dcx RNAi = 212 ± 18 μm, Dcx GOF = 195 ± 25 μm; right graph: control = 2.8 ± 0.2/cell, Dcx RNAi = 3.0 ± 0.2/cell, Dcx GOF = 3.1 ± 0.2/cell; n = 20 cells in each line from three individuals).

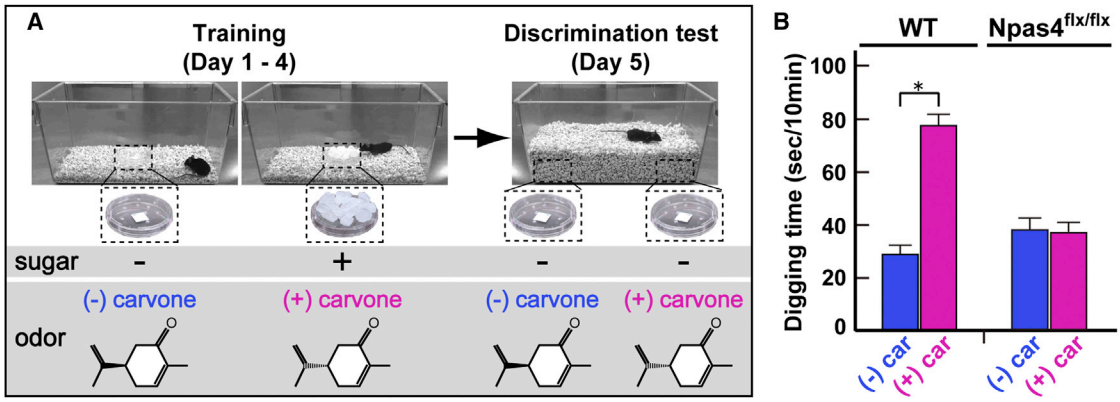

Figure 7. Discrimination Learning with Two Structurally Related Odorants

(A) The odor discrimination learning test with two related odorants: (+) carvone and (−) carvone. Wild-type and *Npas4*$^{flx/flx}$ mice showing OB-specific *Cre* expression were trained for 4 days to associate a reward (sugar grains) with (+) carvone. On day 5, the sugar reward was removed and the time when the mice spent digging in the vicinity of each odorant was measured.

(B) Digging times during the 10 min test period are represented as bar graphs: (+) carvone paired with the sugar reward is shown in pink and unpaired (−) carvone is shown in blue. Digging times are expressed as the mean ± SEM (wild-type: (−) carvone = 29 ± 7 s, (+) carvone = 77 ± 6 s; *Npas4*$^{flx/flx}$: (−) carvone = 37 ± 7 s, (+) carvone = 35 ± 8 s; *p < 0.05 compared with (−) carvone [a one-way ANOVA]; n = 4 individuals for each line).

dendritic spine density of the OB GCs following sensory input. Interestingly, *Dcx* expression is decreased in older GCs. *Npas4* overexpression and knockdown experiments suggest that Npas4 does not regulate the spine formation in mature, older GCs. Recently, it has been reported that younger GCs show a high level of filopodia formation and retraction on the distal dendrites, but this dendritic dynamics is decreased as GCs matured (Breton-Provencher et al., 2014). We speculate that the activity-dependent spine development of GCs is divided into two stages: early and late. Early spine development in young GCs is Npas4-dependent and Dcx-mediated (this study), whereas late spine development in old GCs may be Npas4- and Dcx-independent (unknown mechanism).

In addition, it was reported that the Dcx homologs, Dcx-like kinases 1 and 2 (Dclk1/Dclk2), regulate the dendritic spine formation of hippocampal neurons (Shin et al., 2013). The microtubule-binding protein Dcx family may play a crucial role in dendritic spine development because Dcx and Dclk1/Dclk2 bind to spinophilin, an actin-binding protein known to regulate spine morphology (Tsukada et al., 2003). Therefore, identification of the proteins that interact with Dcx will be important for elucidating the mechanisms that regulate dendritic synapse development in the newborn OB interneurons, which are likely to be linked to the modulation of ubiquitination and proteasome degradation, depending on the sensory input.

What Is the Functional Significance of the Integration of Newborn Neurons into the OB?

Olfactory experience such as odor enrichment and odor learning can regulate the maturation and survival of adult-born OB interneurons. Because newborn OB interneurons show specific properties that differ from those of preexisting interneurons, such as enhanced synaptic plasticity during a critical time window, it is generally thought that they should make a unique contribution to odor processing. However, none of the existing methodologies, such as different ways of physically and genetically eliminating newborn cells, can fully and selectively block the birth of adult-born OB interneurons in a spatially and temporally specific manner (Breton-Provencher et al., 2009; Enwere et al., 2004; Gheusi et al., 2000; Imayoshi et al., 2008; Lazarini et al., 2009; Sultan et al., 2010). By contrast, our genetic approach demonstrates that conditional knockout of *Npas4* function in OB neurons impairs the acquisition of two-related-odors discrimination task (Figure 7). A similar observation was made in an optogenetic study in which channelrhodopsin-2 was selectively expressed in adult-born GCs; light-activation of these newborn neurons facilitated two-related-odors discrimination learning and improved odor memory (Alonso et al., 2012). Collectively, our results may provide evidence that newborn OB interneurons, in which spine formation is regulated by Npas4 in a sensory-experience-dependent manner, contribute to the functioning of olfactory circuits and to the behavioral outcomes that depend upon them.

EXPERIMENTAL PROCEDURES

Detailed procedures are provided in Supplemental Experimental Procedures.

Mice and the Naris Occlusion Procedure

Animal research was approved by the campus committees of Nara Medical University and Nagoya University and was conducted in accordance with its guidelines. ICR and C57BL/6 male and female mice were purchased from Japan SLC. Olfactory sensory deprivation was performed by means of naris occlusion. Newborn mice at P0 were anesthetized with ice and then underwent unilateral cauterization of a nostril with a soldering iron.

Npas4 Mutant Mice

Npas4 mutant mice, in which the *Npas4* gene locus was replaced with *GFP*, and *Npas4*$^{flx/flx}$ mutant mice, in which the *Npas4* coding region was flanked by *loxP* sites, were generously provided by Dr. M. E. Greenberg (Harvard Medical School) (Lin et al., 2008). *Npas4*$^{+/-}$ and *Npas4*$^{-/-}$ littermate and

Npas4$^{flx/-}$ and *Npas4*$^{flx/flx}$ littermate mice were bred from heterozygotes and genotyped as described previously (Lin et al., 2008).

Generation and Injection of Lentiviral Vectors

The procedures used to generate and inject the lentiviral vectors have been previously described (Yoshihara et al., 2012).

Odorant Exposure

P21 mice were habituated in a clean cage without food and water for 2 hr before odorant exposure. Undiluted amyl acetate (60 μl; Nacalai Tesque) was poured onto filter paper in a 1.5 ml microcentrifuge tube that had been cut 1 cm from the base. Mice were exposed to the odorant in the tube without direct contact with the paper for 30 min and were then immediately sacrificed.

In Situ Hybridization

ISH and double ISH were performed as previously described (Serizawa et al., 2006; Tsuboi et al., 1999; Yoshihara et al., 2012).

Immunohistochemistry

IHC of mouse OB sections was performed as previously described (Yoshihara et al., 2005, 2012).

Chromatin Immunoprecipitation Sequencing

ChIP-seq was performed using previously validated methods (Maze et al., 2011).

Isobaric Tags for Relative and Absolute Quantitation

iTRAQ was performed by using previously validated methods (Casey et al., 2010).

Western Blot Analysis of OB Lysates

P21 mice were sacrificed, and isolated OBs were lysed in radioimmunoprecipitation assay (RIPA) buffer (0.1% SDS, 0.5% deoxycholic acid, 1% Triton X-100, 50 mM Tris-HCl, 2 mM EDTA, 150 mM NaCl, phosphatase inhibitors, and protease inhibitors), as previously described (Colledge et al., 2003). OB lysates were separated by SDS-PAGE on a 5%–20% gradient gel (Nacalai Tesque) and transferred to polyvinylidene di fluoride membranes (Merck Millipore). For WB analysis, the following antibodies were used: goat anti-Dcx antibody (1:1,000; Santa Cruz Biotechnology); mouse anti-PSD95 monoclonal antibody (1:40,000; Thermo Fisher Scientific); mouse anti-GAPDH monoclonal antibody (1:40,000; Merck Millipore); donkey anti-goat immunoglobulin G (IgG)-horseradish peroxidase (HRP) (1:20,000; Jackson ImmunoResearch); and donkey anti-mouse IgG-HRP (1:20,000; Jackson ImmunoResearch). Immunoreactive bands were visualized by Chemi-Lumi One L (Nacalai Tesque) and captured on autoradiography films (Hyperfilm Blue; GE Healthcare).

Immunoprecipitation of HEK293 Cell Lysates

The human embryonic kidney cell line HEK293T was transfected at 60%–80% confluency in 3.5 cm^2 plates using Lipofectamine 2000 (Life Technologies). The following plasmids were used: *CAGp—mCherry* (0.5 μg); *CAGp—Dcx* (0.1, 0.5, or 1.0 μg); *CAGp—Mdm2* (1.0 μg); and *CAGp—HA-Ub* (0.5 μg). The *HA-Ub* construct was prepared as previously described (Treier et al., 1994). Cells were harvested and lysed 24 hr after transfection in 500 μl of RIPA buffer, as described above. Cell extracts (100 μg) were incubated with 1 μg of each antibody at 4°C overnight and immunoprecipitated with 25 μl of Dynabeads Protein G (Life Technologies), according to the manufacturer's protocol. After washing three times, bound proteins were eluted with Laemmli sample buffer and analyzed by WB analysis. The following antibodies were used: mouse anti-Mdm2 antibody (1:2,000; Merck Millipore); goat anti-Dcx antibody (1:1,000; Santa Cruz Biotechnology); rat anti-red fluorescent protein (1:1,000; Chromo-Tek); and rabbit anti-HA (1:2,000; Abcam). HRP-conjugated secondary antibodies (1:20,000) were purchased from Jackson ImmunoResearch.

Odor Discrimination Learning Test

A lentiviral vector carrying the *CMVp—Cre—IRES—gapEYFP* construct was injected into both the LVs and OBs of wild-type and *Npas4*$^{flx/flx}$ mice (Lin et al., 2008) at P3. After 6 weeks (P45), odor discrimination learning was tested in wild-type and *Npas4*$^{flx/flx}$ mice, as previously described (Imayoshi et al., 2008).

Statistical Analyses

The total length and spine density of the GC dendrites and *Npas4* hybridization-signal intensities were analyzed with Image-J software (NIH). The total length of the dendrites was defined as the sum of all the dendritic branches from a single neuron. A dendritic process had to be at least 10 μm long to be considered as a branch. The number of dendritic spines was counted manually and divided by the dendrite length to obtain a value for the spine density. According to the method of Scotto-Lomassese et al., (2011), we categorized "spines" as all protrusions with or without a clearly visible head, thereby including filopodia. We defined the proximal region as that from the soma to the first branching point of the apical dendrites and the distal region as that from the branching point to the dendritic tip. All data were analyzed with Microsoft Excel using a one-way ANOVA. Descriptive statistics were displayed as the mean ± SEM. Differences were deemed significant when $p < 0.05$.

SUPPLEMENTAL INFORMATION

Supplemental Information includes Supplemental Experimental Procedures, seven figures, and two tables and can be found with this article online at http://dx.doi.org/10.1016/j.celrep.2014.06.056.

AUTHOR CONTRIBUTIONS

S.Y., H.T., and A.T. designed the experiments. The experiments and data analyses were performed mainly by S.Y. and H.T. and partially by N.N., M. Kinoshita, R.A., M. Kitsuki, and K.T. H.H. constructed the lentiviral vector system. Y.F.-H., T.N., and K.Y. generated the antibodies against mouse Npas4. S.Y., H.T., and A.T. wrote the manuscript. S.Y. and H.T. contributed equally to this work.

ACKNOWLEDGMENTS

This work was supported by Grants-in-Aid for Scientific Research for (B) (A.T.) and (C) (H.T. and S.Y.) and Challenging Exploratory Research (A.T.) from the Ministry of Education, Culture, Sports, Science and Technology (MEXT), Japan. A.T. was supported by grants from the SKYLARK Food Science Institute, Uehara Memorial, Smoking Research, Asahi Research Promotion, and Yamada Science Foundations, Japan. S.Y. and H.T. were supported by grants from Takeda Science Foundation and Astellas Foundation for Research on Metabolic Disorders, Japan. H.T. was supported by a grant from the Salt Science Research Foundation (no. 14C3), Japan. We gratefully thank M. E. Greenberg for the generous gift of the *Npas4* mutant mice and the animal facility staff of Nara Medical University and Nagoya University for their expert assistance.

Received: February 15, 2014
Revised: June 5, 2014
Accepted: June 26, 2014
Published: July 31, 2014

REFERENCES

Adam, Y., and Mizrahi, A. (2010). Circuit formation and maintenance—perspectives from the mammalian olfactory bulb. Curr. Opin. Neurobiol. *20*, 134–140.

Alonso, M., Lepousez, G., Sebastien, W., Bardy, C., Gabellec, M.M., Torquet, N., and Lledo, P.M. (2012). Activation of adult-born neurons facilitates learning and memory. Nat. Neurosci. *15*, 897–904.

Bardy, C., Alonso, M., Bouthour, W., and Lledo, P.M. (2010). How, when, and where new inhibitory neurons release neurotransmitters in the adult olfactory bulb. J. Neurosci. *30*, 17023–17034.

Belvindrah, R., Nissant, A., and Lledo, P.M. (2011). Abnormal neuronal migration changes the fate of developing neurons in the postnatal olfactory bulb. J. Neurosci. *31*, 7551–7562.

Bepari, A.K., Watanabe, K., Yamaguchi, M., Tamamaki, N., and Takebayashi, H. (2012a). Visualization of odor-induced neuronal activity by immediate early gene expression. BMC Neurosci. *13*, 140.

Bepari, A.K., Sano, H., Tamamaki, N., Nambu, A., Tanaka, K.F., and Takebayashi, H. (2012b). Identification of optogenetically activated striatal medium spiny neurons by Npas4 expression. PLoS ONE *7*, e52783.

Bloodgood, B.L., Sharma, N., Browne, H.A., Trepman, A.Z., and Greenberg, M.E. (2013). The activity-dependent transcription factor NPAS4 regulates domain-specific inhibition. Nature *503*, 121–125.

Breton-Provencher, V., Lemasson, M., Peralta, M.R., 3rd, and Saghatelyan, A. (2009). Interneurons produced in adulthood are required for the normal functioning of the olfactory bulb network and for the execution of selected olfactory behaviors. J. Neurosci. *29*, 15245–15257.

Breton-Provencher, V., Coté, D., and Saghatelyan, A. (2014). Activity of the principal cells of the olfactory bulb promotes a structural dynamic on the distal dendrites of immature adult-born granule cells via activation of NMDA receptors. J. Neurosci. *34*, 1748–1759.

Brown, J.P., Couillard-Després, S., Cooper-Kuhn, C.M., Winkler, J., Aigner, L., and Kuhn, H.G. (2003). Transient expression of doublecortin during adult neurogenesis. J. Comp. Neurol. *467*, 1–10.

Casey, T., Solomon, P.S., Bringans, S., Tan, K.C., Oliver, R.P., and Lipscombe, R. (2010). Quantitative proteomic analysis of G-protein signalling in Stagonospora nodorum using isobaric tags for relative and absolute quantification. Proteomics *10*, 38–47.

Colledge, M., Snyder, E.M., Crozier, R.A., Soderling, J.A., Jin, Y., Langeberg, L.K., Lu, H., Bear, M.F., and Scott, J.D. (2003). Ubiquitination regulates PSD-95 degradation and AMPA receptor surface expression. Neuron *40*, 595–607.

Enwere, E., Shingo, T., Gregg, C., Fujikawa, H., Ohta, S., and Weiss, S. (2004). Aging results in reduced epidermal growth factor receptor signaling, diminished olfactory neurogenesis, and deficits in fine olfactory discrimination. J. Neurosci. *24*, 8354–8365.

Gheusi, G., Cremer, H., McLean, H., Chazal, G., Vincent, J.D., and Lledo, P.M. (2000). Importance of newly generated neurons in the adult olfactory bulb for odor discrimination. Proc. Natl. Acad. Sci. USA *97*, 1823–1828.

Imayoshi, I., Sakamoto, M., Ohtsuka, T., Takao, K., Miyakawa, T., Yamaguchi, M., Mori, K., Ikeda, T., Itohara, S., and Kageyama, R. (2008). Roles of continuous neurogenesis in the structural and functional integrity of the adult forebrain. Nat. Neurosci. *11*, 1153–1161.

Kaneko, N., Marín, O., Koike, M., Hirota, Y., Uchiyama, Y., Wu, J.Y., Lu, Q., Tessier-Lavigne, M., Alvarez-Buylla, A., Okano, H., et al. (2010). New neurons clear the path of astrocytic processes for their rapid migration in the adult brain. Neuron *67*, 213–223.

Katz, L.C., and Shatz, C.J. (1996). Synaptic activity and the construction of cortical circuits. Science *274*, 1133–1138.

Kelsch, W., Lin, C.W., Mosley, C.P., and Lois, C. (2009). A critical period for activity-dependent synaptic development during olfactory bulb adult neurogenesis. J. Neurosci. *29*, 11852–11858.

Kim, T.K., Hemberg, M., Gray, J.M., Costa, A.M., Bear, D.M., Wu, J., Harmin, D.A., Laptewicz, M., Barbara-Haley, K., Kuersten, S., et al. (2010). Widespread transcription at neuronal activity-regulated enhancers. Nature *465*, 182–187.

Lazarini, F., Mouthon, M.A., Gheusi, G., de Chaumont, F., Olivo-Marin, J.C., Lamarque, S., Abrous, D.N., Boussin, F.D., and Lledo, P.M. (2009). Cellular and behavioral effects of cranial irradiation of the subventricular zone in adult mice. PLoS ONE *4*, e7017.

Lepousez, G., Valley, M.T., and Lledo, P.M. (2013). The impact of adult neurogenesis on olfactory bulb circuits and computations. Annu. Rev. Physiol. *75*, 339–363.

Lin, Y., Bloodgood, B.L., Hauser, J.L., Lapan, A.D., Koon, A.C., Kim, T.K., Hu, L.S., Malik, A.N., and Greenberg, M.E. (2008). Activity-dependent regulation of inhibitory synapse development by Npas4. Nature *455*, 1198–1204.

Lin, C.W., Sim, S., Ainsworth, A., Okada, M., Kelsch, W., and Lois, C. (2010). Genetically increased cell-intrinsic excitability enhances neuronal integration into adult brain circuits. Neuron *65*, 32–39.

Livneh, Y., Feinstein, N., Klein, M., and Mizrahi, A. (2009). Sensory input enhances synaptogenesis of adult-born neurons. J. Neurosci. *29*, 86–97.

Lledo, P.M., Merkle, F.T., and Alvarez-Buylla, A. (2008). Origin and function of olfactory bulb interneuron diversity. Trends Neurosci. *31*, 392–400.

Maya-Vetencourt, J.F., Tiraboschi, E., Greco, D., Restani, L., Cerri, C., Auvinen, P., Maffei, L., and Castrén, E. (2012). Experience-dependent expression of NPAS4 regulates plasticity in adult visual cortex. J. Physiol. *590*, 4777–4787.

Maze, I., Feng, J., Wilkinson, M.B., Sun, H., Shen, L., and Nestler, E.J. (2011). Cocaine dynamically regulates heterochromatin and repetitive element unsilencing in nucleus accumbens. Proc. Natl. Acad. Sci. USA *108*, 3035–3040.

Nithianantharajah, J., and Hannan, A.J. (2006). Enriched environments, experience-dependent plasticity and disorders of the nervous system. Nat. Rev. Neurosci. *7*, 697–709.

Ooe, N., Saito, K., Mikami, N., Nakatuka, I., and Kaneko, H. (2004). Identification of a novel basic helix-loop-helix-PAS factor, NXF, reveals a Sim2 competitive, positive regulatory role in dendritic-cytoskeleton modulator drebrin gene expression. Mol. Cell. Biol. *24*, 608–616.

Ploski, J.E., Monsey, M.S., Nguyen, T., DiLeone, R.J., and Schafe, G.E. (2011). The neuronal PAS domain protein 4 (Npas4) is required for new and reactivated fear memories. PLoS ONE *6*, e23760.

Pruunsild, P., Sepp, M., Orav, E., Koppel, I., and Timmusk, T. (2011). Identification of cis-elements and transcription factors regulating neuronal activity-dependent transcription of human BDNF gene. J. Neurosci. *31*, 3295–3308.

Qiu, J., Tan, Y.W., Hagenston, A.M., Martel, M.A., Kneisel, N., Skehel, P.A., Wyllie, D.J., Bading, H., and Hardingham, G.E. (2013). Mitochondrial calcium uniporter Mcu controls excitotoxicity and is transcriptionally repressed by neuroprotective nuclear calcium signals. Nat. Commun. *4*, 2034.

Ramamoorthi, K., Fropf, R., Belfort, G.M., Fitzmaurice, H.L., McKinney, R.M., Neve, R.L., Otto, T., and Lin, Y. (2011). Npas4 regulates a transcriptional program in CA3 required for contextual memory formation. Science *334*, 1669–1675.

Rochefort, C., Gheusi, G., Vincent, J.D., and Lledo, P.M. (2002). Enriched odor exposure increases the number of newborn neurons in the adult olfactory bulb and improves odor memory. J. Neurosci. *22*, 2679–2689.

Saghatelyan, A., Roux, P., Migliore, M., Rochefort, C., Desmaisons, D., Charneau, P., Shepherd, G.M., and Lledo, P.M. (2005). Activity-dependent adjustments of the inhibitory network in the olfactory bulb following early postnatal deprivation. Neuron *46*, 103–116.

Sakamoto, M., Imayoshi, I., Ohtsuka, T., Yamaguchi, M., Mori, K., and Kageyama, R. (2011). Continuous neurogenesis in the adult forebrain is required for innate olfactory responses. Proc. Natl. Acad. Sci. USA *108*, 8479–8484.

Sanes, J.R., and Lichtman, J.W. (2001). Induction, assembly, maturation and maintenance of a postsynaptic apparatus. Nat. Rev. Neurosci. *2*, 791–805.

Scotto-Lomassese, S., Nissant, A., Mota, T., Néant-Féry, M., Oostra, B.A., Greer, C.A., Lledo, P.M., Trembleau, A., and Caillé, I. (2011). Fragile X mental retardation protein regulates new neuron differentiation in the adult olfactory bulb. J. Neurosci. *31*, 2205–2215.

Serizawa, S., Miyamichi, K., Takeuchi, H., Yamagishi, Y., Suzuki, M., and Sakano, H. (2006). A neuronal identity code for the odorant receptor-specific and activity-dependent axon sorting. Cell *127*, 1057–1069.

Shin, E., Kashiwagi, Y., Kuriu, T., Iwasaki, H., Tanaka, T., Koizumi, H., Gleeson, J.G., and Okabe, S. (2013). Doublecortin-like kinase enhances dendritic remodelling and negatively regulates synapse maturation. Nat. Commun. *4*, 1440.

Sultan, S., Mandairon, N., Kermen, F., Garcia, S., Sacquet, J., and Didier, A. (2010). Learning-dependent neurogenesis in the olfactory bulb determines long-term olfactory memory. FASEB J. *24*, 2355–2363.

Treier, M., Staszewski, L.M., and Bohmann, D. (1994). Ubiquitin-dependent c-Jun degradation in vivo is mediated by the delta domain. Cell *78*, 787–798.

Tsuboi, A., Yoshihara, S., Yamazaki, N., Kasai, H., Asai-Tsuboi, H., Komatsu, M., Serizawa, S., Ishii, T., Matsuda, Y., Nagawa, F., and Sakano, H. (1999). Olfactory neurons expressing closely linked and homologous odorant receptor genes tend to project their axons to neighboring glomeruli on the olfactory bulb. J. Neurosci. *19*, 8409–8418.

Tsukada, M., Prokscha, A., Oldekamp, J., and Eichele, G. (2003). Identification of neurabin II as a novel doublecortin interacting protein. Mech. Dev. *120*, 1033–1043.

Whitman, M.C., and Greer, C.A. (2009). Adult neurogenesis and the olfactory system. Prog. Neurobiol. *89*, 162–175.

Yamaguchi, M., and Mori, K. (2005). Critical period for sensory experience-dependent survival of newly generated granule cells in the adult mouse olfactory bulb. Proc. Natl. Acad. Sci. USA *102*, 9697–9702.

Yoshihara, S., Omichi, K., Yanazawa, M., Kitamura, K., and Yoshihara, Y. (2005). Arx homeobox gene is essential for development of mouse olfactory system. Development *132*, 751–762.

Yoshihara, S., Takahashi, H., Nishimura, N., Naritsuka, H., Shirao, T., Hirai, H., Yoshihara, Y., Mori, K., Stern, P.L., and Tsuboi, A. (2012). 5T4 glycoprotein regulates the sensory input-dependent development of a specific subtype of newborn interneurons in the mouse olfactory bulb. J. Neurosci. *32*, 2217–2226.

Yun, J., Koike, H., Ibi, D., Toth, E., Mizoguchi, H., Nitta, A., Yoneyama, M., Ogita, K., Yoneda, Y., Nabeshima, T., et al. (2010). Chronic restraint stress impairs neurogenesis and hippocampus-dependent fear memory in mice: possible involvement of a brain-specific transcription factor Npas4. J. Neurochem. *114*, 1840–1851.